

· 基础研究 ·

改良球囊损伤联合高脂饮食建立兔腹主动脉粥样硬化模型

华芮,李宸,雍辉,林清霞,董舟,吕展*,李春坚*

南京医科大学第一附属医院心内科,江苏 南京 210029

[摘要] **目的:**评估改良球囊损伤联合高脂饮食建立兔腹主动脉粥样硬化模型方法的有效性,并检测早期斑块中免疫清除相关蛋白的表达。**方法:**采用20只新西兰大白兔,随机分为假手术组、经典手术组、改良手术组。假手术组予普通饮食,麻醉、切皮、分离股动脉加缝合,但不行球囊损伤。经典手术组和改良手术组予高脂饮食1周后,行腹主动脉球囊损伤术,其中经典手术组单向拉动球囊3次,改良手术组反复前后拉动球囊30~40次,术后继续高脂饮食4周。术后4周采用血管内超声检查腹主动脉内膜斑块情况,取腹主动脉损伤段行苏木素-伊红(hematoxylin-eosin, HE)染色和免疫组化检测。**结果:**术后4周,各组体重增加差异无统计学意义。血管内超声显示改良手术组斑块增生显著,管腔狭窄。HE染色显示经典手术组和改良手术组均有不同程度的内膜增生,造模成功率均为100%。与经典手术组相比,改良手术组最大内膜厚度[(174.69±53.76) μm vs. (481.50±81.94) μm, $P < 0.05$]、平均内膜厚度[(77.49±18.02) μm vs. (262.63±53.04) μm, $P < 0.05$]、内膜中膜面积比[0.39±0.14 vs. 1.57±0.30, $P < 0.05$]和血管狭窄比例[(19.04±5.90)% vs. (52.13±11.31)%, $P < 0.05$]均显著增加,免疫组化提示改良手术组较经典手术组巨噬细胞浸润更为显著。相比假手术组和经典手术组,改良手术组增生内膜中抗吞噬蛋白CD47表达更为显著。**结论:**改良球囊损伤联合高脂饮食建立兔腹主动脉粥样硬化模型的方法进一步加速了斑块进展,造模更稳定,可靠性更高,且在早期斑块中即可观察到显著的坏死细胞清除缺陷。

[关键词] 动脉粥样硬化;兔;球囊损伤改良术;CD47**[中图分类号]** R543.5**[文献标志码]** A**[文章编号]** 1007-4368(2024)03-322-07**doi:** 10.7655/NYDXBNSN230774

Construction of a rabbit model of abdominal aorta atherosclerosis by a modified balloon injury with a high-cholesterol diet

HUA Rui, LI Chen, YONG Hui, LIN Qingxia, DONG Zhou, LÜ Zhan*, LI Chunjian*

Department of Cardiology, the First Affiliated Hospital of Nanjing Medical University, Nanjing 210029, China

[Abstract] **Objective:** To construct a rabbit model of abdominal aorta atherosclerosis by a modified balloon injury with a high-cholesterol diet, and evaluate the expression of immune clearance related proteins in early plaques. **Methods:** A total of 20 New Zealand rabbits were assigned randomly to 3 groups: a sham group, a classical intervention group and a modified intervention group. The high-cholesterol diet and normal diet were given to the intervention groups and the sham group, respectively for one week, after which the model was constructed through the femoral artery. The rabbits in the sham group were given a general diet, anesthetized, skin cut, isolated femoral artery and sutured, but without balloon injury. For the rabbits in the classic intervention group, a balloon was inserted into the abdominal aorta, inflated and unidirectionally pulled 3 times. For the rabbits in the modified intervention group, the balloon was inserted, inflated and a bidirectionally pushed and pulled for 30–40 times. Following the intervention, the two intervention groups received a high-cholesterol diet, while the sham group received a normal diet for another 4 weeks. The intravascular ultrasound was performed to examine the abdominal aorta *via* the femoral artery, and the injured segments of abdominal aorta were sampled for further hematoxylin-eosin (HE) and immunohistochemistry staining at the end of the study. **Results:** There was no significant difference in weight gain measured at 4 weeks post intervention among the 3 groups. The intravascular ultrasound demonstrated significant plaque hyperplasia and lumen stenosis in the modified intervention group. HE staining revealed varying degrees of intimal hyperplasia in all samples from both intervention groups. Compared with the classical intervention group, the modified intervention

[基金项目] 国家重点研发计划(2022YFC2402404);中国博士后科学基金面上资助项目(2023M731411)

*通信作者(Corresponding author), E-mail: lijay@njmu.edu.cn; lvzhan1995@163.com

group exhibited significantly increased in maximum intimal thickness [(174.69±53.76) μm vs. (481.50±81.94) μm , $P < 0.05$] and mean intimal thickness [(77.49±18.02) μm vs. (262.63±53.04) μm , $P < 0.05$], a higher intimal /media area ratio [0.39±0.14 vs. 1.57±0.30, $P < 0.05$] and severer vascular stenosis [(19.04±5.90)% vs. (52.13±11.31)% , $P < 0.05$]. The immunohistochemistry staining revealed significantly enhanced macrophage infiltration in the modified intervention group, compared with the classical intervention group. Moreover, a higher expression of the anti-phagocytic protein CD47 in the proliferative intima was detected in the modified intervention group than the sham group and the classical intervention group. **Conclusion:** The novel rabbit model of abdominal aorta atherosclerosis was established by the modified balloon injury and the high - cholesterol diet, further accelerating early plaque development with an enhanced stability and reliability. A significant necrotic cell clearance impairment was detected in early plaque in this novel model.

[Key words] atherosclerosis; rabbit; modified balloon injury; CD47

[J Nanjing Med Univ, 2024, 44(03):322-328]

动脉粥样硬化(atherosclerosis, AS)是一种以脂质代谢障碍为基础、血管内壁脂质沉积为特征的慢性、进行性动脉血管病变,严重危害人类生命健康^[1-3]。AS斑块破裂,可继发血栓形成,从而造成组织严重缺血、缺氧、甚至坏死^[4-5]。建立动物模型,进一步研究AS的发病机制,对预防心血管事件有重要意义。

兔是建立AS模型常用的动物之一。目前研究多采用球囊损伤联合高脂饮食建立兔腹主动脉粥样硬化模型,这在一定程度上避免了单纯高脂饮食带来的耗时长、动物多脏器脂质沉积等缺陷,但仍存在建模时间长、动物死亡率高、模型不稳定等问题^[6]。本研究采用一种改良的球囊损伤方式、联合4周高脂饮食建立兔腹主动脉粥样硬化模型,探讨其与经典手术方式在模型成功率、稳定性和斑块发展速度等方面的差异。

分化簇(cluster of differentiation, CD)47,也称为整合素相关蛋白,是广泛表达于细胞膜表面的抑制性受体,在免疫系统的自我识别中起关键作用^[7]。CD47与巨噬细胞上的信号调节蛋白 α (signal regulatory protein alpha, SIRP α)跨膜蛋白结合,向巨噬细胞传递吞噬抑制信号^[8]。研究报道CD47在小鼠和人类AS斑块的内膜和平滑肌中的表达显著上调^[9-10]。然而,CD47是否在早期AS斑块中表达并损害吞噬清除作用尚缺乏研究。本研究将利用建立的兔腹主动脉早期粥样硬化模型,验证CD47在AS早期斑块中的表达,为AS的发病机制和治疗研究提供借鉴。

1 材料和方法

1.1 材料

Maverick™2.0 mm×15.0 mm 球囊(Boston Scientific 公司,美国), Quantum™3.5 mm×15.0 mm 球囊(Boston Scientific 公司,美国), PILOT 50 导丝(Ab-

bott Vascular 公司,美国); 压力泵(Merit 公司,美国), 血管内超声(intravascular ultrasound, IVUS)仪(Volcano 公司,美国); 苏木素染色液(武汉赛维尔生物公司), 伊红染色液(武汉赛维尔生物公司); CD47 抗体(北京博奥森生物公司), CD68 抗体(Thermo Fisher Scientific 公司,美国); 丙泊酚乳状注射液(北京费森尤斯卡比公司); 利多卡因注射液(重庆天圣药业有限公司); 青霉素(石家庄华北制药股份有限公司)。

1.2 方法

1.2.1 动物与饲养

3月龄健康雄性新西兰白兔20只,体重2.0~2.5 kg,由南京市莱芙养殖场提供[许可证编号:SCXK(苏)2019-0005,合格证号:202238952]。所有动物单笼饲养,自由饮水,保持12 h昼夜节律,恒定温度和湿度,本研究方案经过南京医科大学实验动物福利伦理委员会审查批准(编号:IACUC-2207041)。手术组15只,根据造模方式又分为经典手术组和改良手术组,麻醉、切皮、分离股动脉,经股动脉随机行经典球囊损伤或改良球囊损伤,术后缝合创口,予高脂饮食4周。假手术组5只,同样麻醉、切皮、分离股动脉加缝合,但不行球囊损伤,术后予普通饮食4周。20只兔术前对应饲料适应性喂养1周。高脂饲料配制:1%胆固醇、8%猪油、7.5%蛋黄粉和83.5%普通饲料。

1.2.2 球囊损伤术构建兔腹主动脉粥样硬化模型

经耳缘静脉注射丙泊酚(6 mg/kg)麻醉,麻醉成功表现为呼吸深慢、四肢瘫软、角膜反射迟缓。将兔仰卧位固定于手术台上,双侧股三角区局部备皮、消毒,利多卡因局部麻醉,在股动脉搏动明显处切口,沿动脉走行方向切开皮肤、逐层分离筋膜肌肉,暴露右股动脉。游离右股动脉4~5 cm,近心端

用丝线套取游离备用,远心端用丝线结扎。近心端用动脉夹夹闭,用眼科剪在远心端剪一“V”形切口。

经典手术方式:将3.5 mm×15.0 mm球囊导管沿导丝送入腹主动脉内,送入过程中松开动脉夹,球囊进入深度约15 cm。将球囊加压至12~14大气压(1 215.6~1 418.2 kPa),回拉球囊导管10 cm,然后球囊减压至0 kPa,再次送至原位置,如此反复3次,损伤腹主动脉内皮。撤出球囊导管,迅速以动脉夹夹闭股动脉,结扎股动脉近心端,松开动脉夹,缝合消毒。

改良手术方式:将2.0 mm×15.0 mm球囊导管沿导丝送入股动脉内约2 cm,以4个大气压(405.2 kPa)扩张球囊,阻断血流,固定球囊,松开动脉夹,继续送入导丝25~30 cm,动脉夹夹闭近心端,撤出球囊。将3.5 mm×15.0 mm球囊导管沿导丝送入腹主动脉内,送入过程中松开动脉夹,球囊进入深度为25~30 cm。将球囊加压至20个大气压(2 026.0 kPa),反复前后拉动球囊30~40次,逐步回撤10 cm,损伤腹主动脉内皮。撤出球囊导管,迅速以动脉夹夹闭股动脉,结扎股动脉近心端,松开动脉夹,缝合消毒。

术后常规护理,予青霉素2 500 U/kg肌注,连续3 d。

1.2.3 IVUS检查

术后各组对应饮食喂养4周,麻醉后暴露切开左侧股三角区,穿刺左股动脉,沿导丝送入IVUS探头,在超声引导下将探头送至降主动脉左肾动脉开口以上水平,采用机器自动控制系统,缓慢匀速回拉超声导管至髂总动脉分叉处,全程记录超声图像,保存供脱机分析。

1.2.4 苏木素-伊红(hematoxylin-eosin, HE)染色

各组兔完成IVUS检测后,沿耳缘静脉注入过量丙泊酚处死两组实验兔,开腹,动脉夹夹闭膈肌下近心端腹主动脉,结扎两侧肾动脉。从降主动脉与肾动脉开口间向下切取约8 cm腹主动脉,取出腹主动脉。切取左肾动脉开口以下约8 cm的腹主动脉,于肝素水中冲洗后,4%多聚甲醛固定24 h。标尺测量切取动脉,每段1 cm,顺序编号后进行石蜡包埋,每层4 μm逐层切片。部分切片HE染色后,拍摄图像,取粥样硬化斑块最大切面,Image J分析计算粥样硬化斑块最大内膜厚度、平均内膜厚度、内膜中膜面积比及血管狭窄比例(斑块面积/管腔总面积)。

1.2.5 免疫组化检测

免疫组化检测假手术组和改良手术组血管中巨噬细胞相关蛋白CD68及抗吞噬蛋白CD47的蛋白表达水平。上述石蜡切片进行脱蜡、水化和蒸馏水冲洗。山羊血清封闭1 h后,切片分别与CD68一

抗(1:50)、CD47一抗(1:400)在4℃孵育过夜。室温下与二抗孵育1 h,用二氨基联苯胺染色,蒸馏水阻断反应,封片后在显微镜下观察拍摄。

1.3 统计学方法

所有数据均以均数±标准差($\bar{x} \pm s$)表示,两组资料之间比较采用独立样本t检验,成组资料采用配对样本t检验,所有统计学结果均采用GraphPad Prism 8进行分析, $P < 0.05$ 为差异有统计学意义。

2 结果

2.1 一般情况

正常饮食假手术组无死亡,手术组当日麻醉死亡1只,动脉夹层破裂死亡1只(改良手术组),高脂饲养过程中绝食重度营养不良死亡1只(经典手术组),剩余12只(经典手术组与改良手术组各6只)均完成4周的高脂饮食喂养,每组均有1只出现轻度趾甲溃烂。各组体重变化见表1,经典手术组与改良手术组体重变化比较,差异无统计学意义(图1)。

2.2 兔腹主动脉IVUS结果

各组兔腹主动脉IVUS图像见图2。假手术组:内膜无增厚,血流通畅,管腔无狭窄;经典手术组:内膜稍增厚模糊,未见管腔明显狭窄与斑块形成;改良手术组:内膜明显增厚,斑块突出于腔内,呈偏心

表1 各组兔造模前后体重

Table 1 The weight of rabbits in each group before and after modeling (kg, $\bar{x} \pm s$)

Weight	Sham group (n=5)	Classical intervention group (n=6)	Modified intervention group (n=6)
Before modeling	2.30 ± 0.11	2.30 ± 0.11	2.30 ± 0.18
After modeling	2.70 ± 0.17	2.80 ± 0.21	2.90 ± 0.13

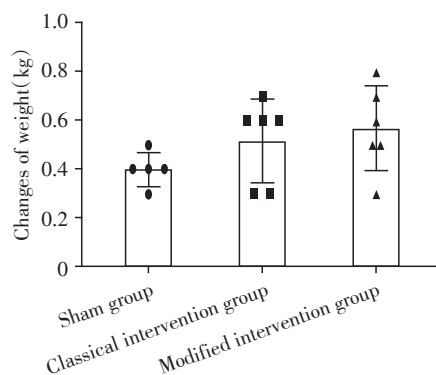


图1 各组兔造模前后体重差值
Figure 1 Weight changes of rabbits in each group before and after modeling

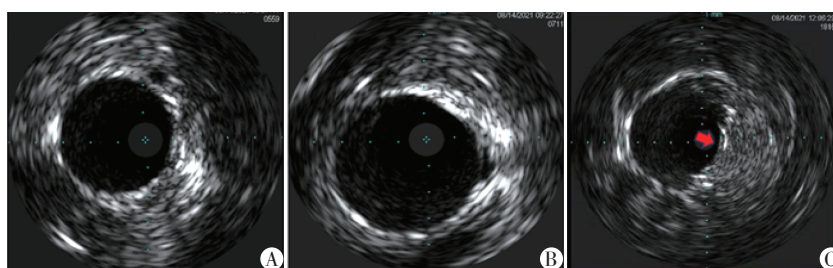
性分布,与管腔分界清晰,回声强度均匀,为内膜增厚回声,与内弹性膜形成的高回声层间分界不清晰,强度低于血管外膜,没有钙化回声,为脂质斑块。

2.3 兔腹主动脉内膜增生情况

各组兔腹主动脉HE染色和巨噬细胞标志物CD68表达情况见图3。假手术组:管腔单层内皮细胞扁平连续,未见增厚,平滑肌细胞整齐有序,细胞核蓝染,胞浆呈红色,各层细胞及弹力膜结构清晰,无脂质沉积。未见棕黄色蛋白,无巨噬细胞沉积。经典手术组:管腔少部分内膜轻度增厚,增厚内膜中多层平滑肌细胞排列紊乱,可见小空泡,少量棕

黄色沉积,巨噬细胞少量浸润,内弹力膜尚清晰。改良手术组:血管纵切面内膜普遍全程不均匀偏心增厚,向管腔凸出,形成斑块。部分内膜断裂,增厚内膜各层细胞紊乱堆叠,胞浆嗜酸红染的平滑肌细胞减少,代之以大量胞浆淡染和充满脂质空泡的泡沫细胞,大量巨噬细胞浸润,各层结构界限模糊,管腔明显狭窄。

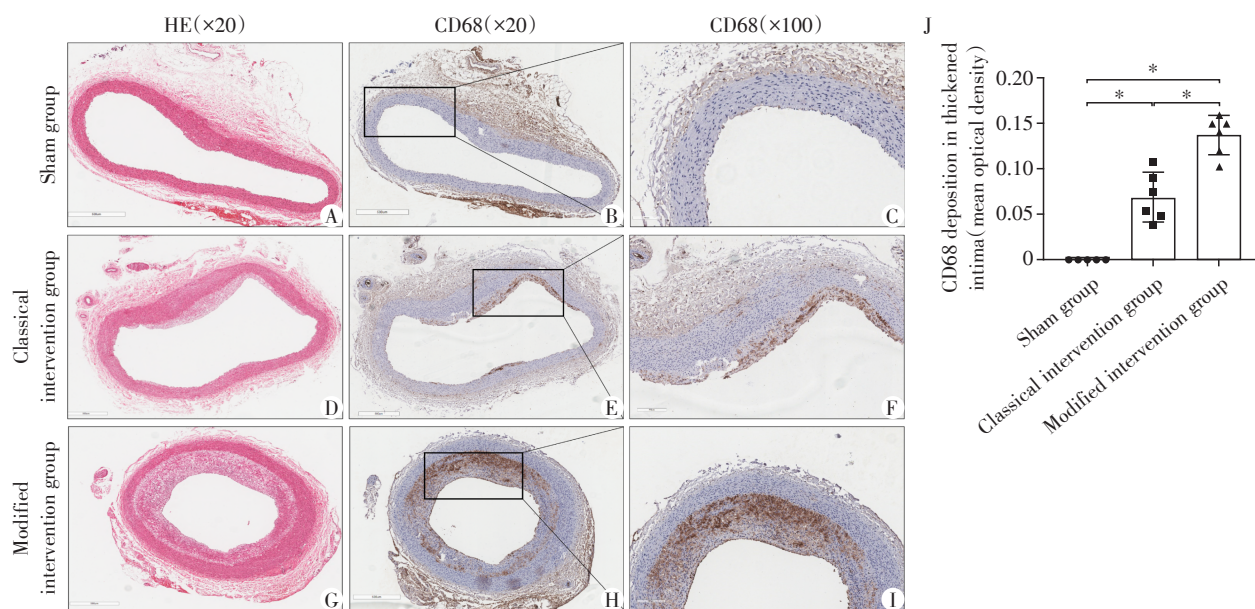
与假手术组比,手术组内膜增厚程度及管腔狭窄比例差异有统计学意义($P < 0.05$)。改良手术组内膜最大厚度、平均内膜厚度、内膜中膜面积比、管腔狭窄比例均大于经典手术组($P < 0.05$,表2)。



A: Sham group with no thickened intima. B: Classical intervention group with a slightly thickened intima. C: Modified intervention group with significantly thickened intima, indicated by the arrow.

图2 术后高脂饮食4周各组兔腹主动脉IVUS影像

Figure 2 IVUS images of abdominal aortas in rabbits of each group after a high-cholesterol diet for 4 weeks



A: HE staining of the sham group with no thickened intima. B, C: Immunohistochemistry of CD68 protein in the sham group with no brownish-yellow deposition. D: HE staining of the classical intervention group with a mild thickened intima in some parts. E, F: Immunohistochemistry of CD68 protein in the classical intervention group with a small number of macrophage infiltration. G: HE staining of the modified intervention group with a significantly uneven intimal hyperplasia. H, I: Immunohistochemistry of CD68 protein in the modified intervention group with a large number of macrophage infiltration. J: The CD68 deposition in thickened intima of each group, $*P < 0.05$.

图3 术后高脂饮食4周各组兔的腹主动脉HE染色及CD68蛋白免疫组化染色

Figure 3 The HE staining and CD68 immunohistochemical staining of abdominal aortas in rabbits of each group after a high-cholesterol diet for 4 weeks

表2 各组兔腹主动脉内膜增生程度

Table 2 The degree of abdominal aorta intima hyperplasia in rabbits of each group ($\bar{x} \pm s$)

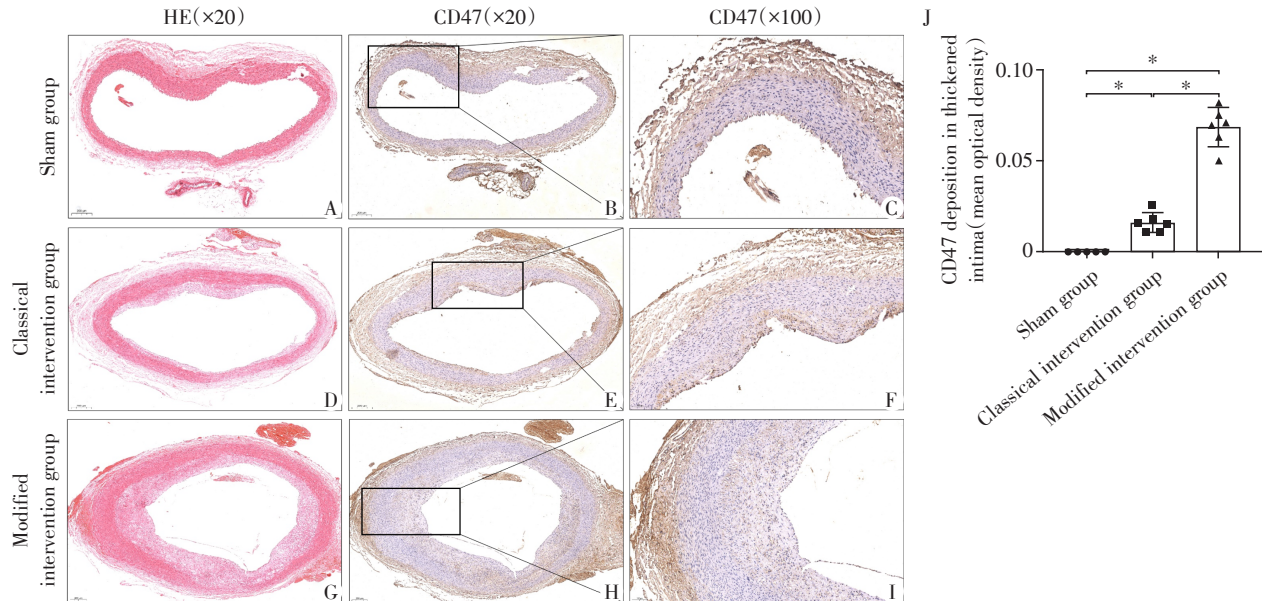
Parameters	Sham group(n=5)	Classical intervention group(n=6)	Modified intervention group(n=6)
Maximum intimal thickness(μm)	32.87 \pm 3.26	174.69 \pm 53.76 [*]	418.5 \pm 81.94 ^{*#}
Mean intimal thickness(μm)	21.76 \pm 1.18	77.49 \pm 18.02 [*]	262.63 \pm 53.04 ^{*#}
Ratio of intima to media area	0.05 \pm 0.01	0.39 \pm 0.14 [*]	1.57 \pm 0.30 ^{*#}
Vascular stenosis(%)	1.99 \pm 0.42	19.04 \pm 5.90 [*]	52.13 \pm 11.31 ^{*#}

Compared with the sham group, ^{*}*P* < 0.05; compared with the classical intervention group, [#]*P* < 0.05.

2.4 早期斑块中 CD47 的表达

各组腹主动脉 HE 染色及斑块中的抗吞噬蛋白 CD47 的免疫组化检测结果见图 4。假手术组的腹主动脉内膜未见棕黄色染色,提示 CD47 低表达或不表达;经典手术组可见少量棕黄色染色团块聚集于增生内膜内,提示斑块内 CD47 低表达;改良手术

组可见棕黄色染色团块聚集于泡沫细胞内,颗粒状弥散性表达于细胞外基质。平滑肌层细胞核蓝染,胞质透明,无棕色沉积,各层界限分明,提示斑块内 CD47 高表达,且局限于增生的内膜。与假手术组和经典手术组比,CD47 在改良手术组的表达差异有统计学意义。



A: HE staining of the sham group with no thickened intima. B, C: Immunohistochemistry of CD47 protein in the sham group with no brownish-yellow deposition in the intima. D: HE staining of the classical intervention group with mild thickened intima in some parts. E, F: Immunohistochemistry of CD47 protein in the classical intervention group with mild brownish-yellow deposition in the intima. G: HE staining of the modified intervention group with significantly uneven intimal hyperplasia. H, I: Immunohistochemistry of CD47 protein in the modified intervention group with extensive brownish-yellow deposition in the intima. J: The CD47 deposition in thickened intima of each group, ^{*}*P* < 0.05.

图4 各组兔腹主动脉 CD47 蛋白免疫组化染色

Figure 4 The CD47 immunohistochemical staining of abdominal aortas in rabbits of each group

3 讨论

兔与人类的血脂代谢极为相似,是最早用于建立 AS 模型动物之一^[11]。单纯高脂饮食造模,造模周期长、慢性并发症较多、模型成功率受个体间差异影响大,实际应用受限^[12-14]。现多采用球囊损伤联合高脂饮食,一定程度上缩短了造模时间,但周

期仍长达 12~16 周,且动物死亡率高,模型稳定性不足^[15-16]。本研究在传统内皮损伤法的基础上进行改良。经典球囊损伤多采用 3.5 mm×15.0 mm 球囊导管 8~14 个大气压(810.4~1 418.2 kPa)扩张后回拉 3 次造成内皮损伤^[17]。在本研究的球囊损伤模型中,首先采用直径 2.0 mm 的球囊进入股动脉,4 个大气压(405.2 kPa)扩张后阻断血流,将导丝沿球囊送

入腹主动脉25~30 cm后更换为直径3.5 mm的球囊,减少了术中出血。内皮损伤阶段应用20个大气压(2 026.0 kPa)扩张球囊,反复前后拉动球囊30~40次,逐步回撤,造成广泛的腹主动脉内皮损伤,且未对兔的术中、术后生存率产生影响。所有手术模型兔均有不同程度的内膜增生,两种手术方案造模成功率均为100%。

陈家元等^[18]建立的高脂饮食联合球囊损伤兔腹主动脉模型中,采用经典手术方式,术后4周腹主动脉处于脂纹阶段,出现轻度内膜增生,8周后出现了造影可见的内膜增生和血管狭窄。本研究改良手术方式后,4周即可在IVUS下观察到显著的内膜增生和血管狭窄,且体重改变与经典手术组的差异无统计学意义,提示改良手术方式可加速AS斑块进展。此外,免疫组化结果显示两种手术方式均有细胞内脂质沉积,巨噬细胞浸润,而无明显钙化、脂质核心或坏死核心,说明斑块均为早期软斑块,而改良手术组的内膜厚度和斑块体积较经典手术组显著增加,造成明显血管狭窄,提示改良后的造模方法周期更短、更稳定,可靠性高。

AS的特点是慢性持续炎症反应和坏死细胞堆积^[19]。在AS早期,巨噬细胞吞噬在损伤内膜下积聚的低密度脂蛋白,形成泡沫细胞并发生细胞死亡。凋亡细胞清除缺陷导致巨噬细胞进一步聚集,与积累的死亡细胞及脂质碎片形成坏死核心,诱发持续炎症反应,加速AS进展,形成晚期AS^[20]。本研究可见巨噬细胞在手术组的斑块内浸润,改良手术组中巨噬细胞浸润显著高于经典手术组,且多在内膜深层堆积。CD47作为阻断巨噬细胞吞噬信号的膜蛋白,因在恶性肿瘤细胞表面过表达,促进肿瘤免疫逃逸而被广泛关注^[21]。Kojima等^[22]在小鼠主动脉和人类颈动脉粥样硬化晚期斑块中也发现了CD47的过度表达,并且在小鼠AS高脂饮食早期应用抗CD47抗体可以显著减少斑块内凋亡细胞数目,缩小斑块体积,促进斑块稳定。本研究首次揭示了兔腹主动脉AS发展早期出现了只局限于增生内膜中的CD47过表达,且CD47在斑块内不同成分中普遍过表达,提示巨噬细胞清除缺陷在AS早期发挥了重要作用。在IVUS可诊断的早期斑块中,抑制CD47可能成为早期抑制AS发展的新策略。

综上,本研究一方面改良了手术方式,加速了斑块进展,4周即形成了IVUS可诊断的明显增生内膜,狭窄程度较一致,适用于AS斑块的快速诱导和早期斑块机制的研究。另一方面,本研究首次揭示了

在兔腹主动脉AS中,抗吞噬分子CD47在斑块早期有显著过表达,该时期抑制CD47,有可能增加坏死细胞清除,为延缓AS进展提供了新的潜在策略。

[参考文献]

- [1] LIBBY P. The changing landscape of atherosclerosis [J]. *Nature*, 2021, 592(7855): 524-533
- [2] TSAO C W, ADAY A W, ALMARZOOQ Z I, et al. Heart disease and stroke statistics - 2023 update: a report from the American Heart Association [J]. *Circulation*, 2023, 147(8): 93-621
- [3] 崔海鹏,林映雪,王怡宁,等. Urantide对动脉粥样硬化大鼠脂肪肝组织中STAT3磷酸化的影响[J]. *南京医科大学学报(自然科学版)*, 2021, 41(1): 29-34
- [4] BJÖRKEGREN J L M, LUSIS A J. Atherosclerosis: recent developments [J]. *Cell*, 2022, 185(10): 1630-1645
- [5] CHEN W, SCHILPEROORT M, CAO Y H, et al. Macrophage-targeted nanomedicine for the diagnosis and treatment of atherosclerosis [J]. *Nat Rev Cardiol*, 2022, 19(4): 228-249
- [6] 冯斌,杨庭树,张华巍. 高脂饲料喂养与动脉内膜球囊损伤结合建立兔腹主动脉粥样硬化模型[J]. *中国组织工程研究与临床康复*, 2009, 13(15): 2911-2914
- [7] HAYAT S M G, BIANCONI V, PIRRO M, et al. CD47: role in the immune system and application to cancer therapy [J]. *Cell Oncol (Dordr)*, 2020, 43(1): 19-30
- [8] LOGTENBERG M E W, SCHEEREN F A, SCHUMACHER T N. The CD47-SIRP α immune checkpoint [J]. *Immunity*, 2020, 52(5): 742-752
- [9] RYAN J J. CD47-blocking antibodies and atherosclerosis [J]. *JACC Basic Transl Sci*, 2016, 1(5): 413-415
- [10] SOLANKI A, BHATT L K, JOHNSTON T P. Evolving targets for the treatment of atherosclerosis [J]. *Pharmacol Ther*, 2018, 187: 1-12
- [11] FAN J L, CHEN Y J, YAN H Z, et al. Principles and applications of rabbit models for atherosclerosis research [J]. *J Atheroscler Thromb*, 2018, 25(3): 213-220
- [12] STURZENEKER M C S, NORONHA L D, OLANDOSKI M, et al. Ramipril significantly attenuates the development of non-alcoholic steatohepatitis in hyperlipidaemic rabbits [J]. *Am J Cardiovasc Dis*, 2019, 9(2): 8-17
- [13] SCHÜRMAN C, DIENST F L, PÁLFI K, et al. The polarity protein Scrib limits atherosclerosis development in mice [J]. *Cardiovasc Res*, 2019, 115(14): 1963-1974
- [14] ZHANG F, ZHANG R Y, ZHANG X Y, et al. Comprehensive analysis of circRNA expression pattern and circRNA-miRNA-mRNA network in the pathogenesis of atherosclerosis in rabbits [J]. *Aging*, 2018, 10(9): 2266-2283
- [15] LIN L J, XIE Z H, XU M Q, et al. IVUS/IVPA hybrid in-

- travascular molecular imaging of angiogenesis in atherosclerotic plaques *via* RGDfk peptide-targeted nanoprobe [J]. *Photoacoustics*, 2021, 22: 100262
- [16] SU T, WANG Y B, HAN D, et al. Multimodality imaging of angiogenesis in a rabbit atherosclerotic model by GEBP11 peptide targeted nanoparticles [J]. *Theranostics*, 2017, 7(19): 4791-4804
- [17] LI R J, CUI S M, XU Y S, et al. The upregulated scavenger receptor CD36 is associated with the progression of nontarget lesions after stent implantation in atherosclerotic rabbits [J]. *J Inflamm Res*, 2018, 11: 447-456
- [18] 陈家元, 张爱东, 卢红艳, 等. 高脂饮食联合球囊内皮损伤术建立兔腹主动脉粥样硬化模型的可行性研究 [J]. *临床心血管病杂志*, 2014, 30(9): 755-758
- [19] ZHANG J, ZHAO X K, GUO Y Y, et al. Macrophage ALDH2 (aldehyde dehydrogenase 2) stabilizing Rac2 is required for efferocytosis internalization and reduction of atherosclerosis development [J]. *Arterioscler Thromb Vasc Biol*, 2022, 42(6): 700-716
- [20] TAJBAKSH A, BIANCONI V, PIRRO M, et al. Efferocytosis and atherosclerosis: regulation of phagocyte function by microRNAs [J]. *Trends Endocrinol Metab*, 2019, 30(9): 672-683
- [21] CAO X, WANG Y Y, ZHANG W C, et al. Targeting macrophages for enhancing CD47 blockade-elicited lymphoma clearance and overcoming tumor-induced immunosuppression [J]. *Blood*, 2022, 139(22): 3290-3302
- [22] KOJIMA Y, VOLKMER J P, MCKENNA K, et al. CD47-blocking antibodies restore phagocytosis and prevent atherosclerosis [J]. *Nature*, 2016, 536(7614): 86-90
- [收稿日期] 2023-08-18
(本文编辑: 陈汐敏)

(上接第 304 页)

- [21] SZWEDOWICZ U, SZEWCZYK A, GOŁĄB K, et al. Evaluation of wound healing activity of salvianolic acid B on *in vitro* experimental model [J]. *Int J Mol Sci*, 2021, 22(14): 7728
- [22] MENG H, ZHAO M M, YANG R Y, et al. Salvianolic acid B regulates collagen synthesis: indirect influence on human dermal fibroblasts through the microvascular endothelial cell pathway [J]. *J Cosmet Dermatol*, 2022, 21(7): 3007-3015
- [23] RECZEK C R, CHANDEL N S. Revisiting vitamin C and cancer [J]. *Science*, 2015, 350(6266): 1317-1318
- [24] HE F, ANTONUCCI L, YAMACHIKA S, et al. NRF₂ activates growth factor genes and downstream AKT signaling to induce mouse and human hepatomegaly [J]. *J Hepatol*, 2020, 72(6): 1182-1195
- [25] 芮国华, 潘荣华, 姚刚, 等. 丹酚酸 B 对 TGF-β1 诱导的人肾小管细胞转分化的影响 [J]. *南京医科大学学报(自然科学版)*, 2009, 29(12): 1685-1689
- [26] 丁超, 谢利平, 李荣成. 丹酚酸 A 对压力超负荷大鼠心功能减退和心室重构的改善作用 [J]. *南京医科大学学报(自然科学版)*, 2014, 34(1): 12-17
- [收稿日期] 2023-10-10
(本文编辑: 陈汐敏)